2.2.2 Model Calibration and Validation

The DRM described above will be calibrated using data acquired in the STW. Geological parameters (e.g., porosity, permeability), fluid flow data (e.g., relative permeability), and initial reservoir data (e.g., temperature, initial pressure gradient, fracture pressure gradient) will be used to calibrate the computational model.

In the absence of data from the STW and to address the range of uncertainty and demonstrate that impact on the DRM, three alternative DRM simulations were completed based on our current understanding of the range of variation of two uncertainty parameters: salinity and relative permeability. Each of these three scenarios is constrained to the same injection rate and only the uncertainty parameter is varied compared to the base case. They consist of 35,00 ppm salinity, 80,000 ppm salinity, and multiple relative permeability curves. Figure 2-23 illustrates the lateral extent of the base case at the end of 50 years of monitoring compared to that of each of the simulated uncertainties. Overall, the model suggests that there is only a slight chance of plume extent variation among the four scenarios (base case included). The following parts of this section will describe the plume in greater details including individual map views, cross sectional views, and post-injection plume dynamics.

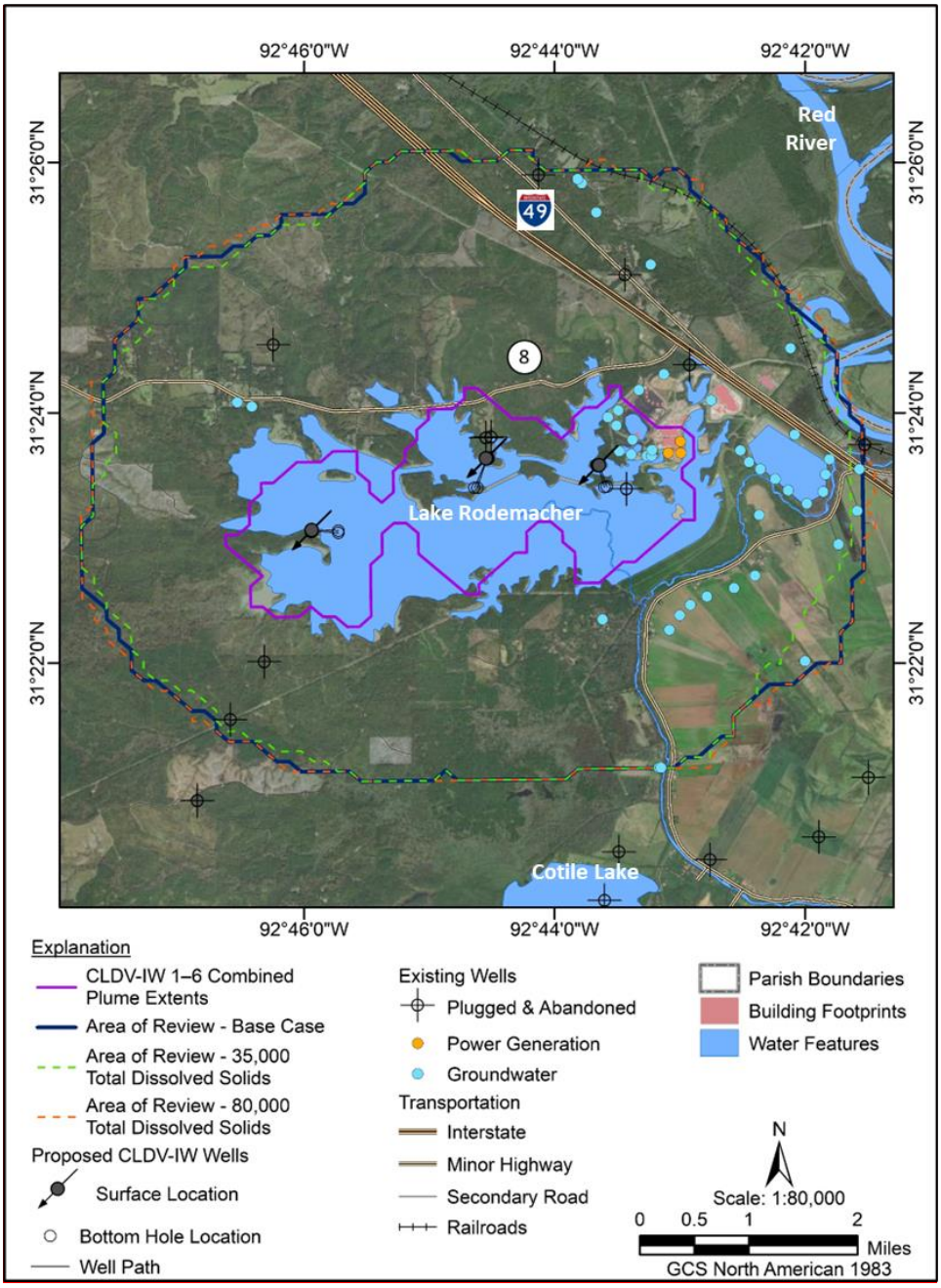

Figure 2-23: Comparison of the base case plume boundary after 12 years of injection (white solid line) versus sensitivity cases including 35,000 ppm salinity (dashed red line), 80,000 ppm salinity (dashed blue line), and multiple relative permeability curves (dashed black line)

Petrophysical evaluation of various well logs in the area suggests that salinity may range from 35,000 to 80,000 ppm. Therefore, two DRM simulations using these end-member values were carried out to estimate the range of response on the injectivity and plume dynamics. The outcome of these runs indicates a low chance of variation in the plume size and overall injectivity.

For salinity at 35,000 ppm, the plume does not differ significantly from the base case during injection (Figure 2-24). However, there may be more plume downward migration (from the cross sectional views through time) as this case is not as saline as the base case (70,000 ppm), which is more helpful for long-term storage safety.

Figure 2-25 describes the post-injection plume dynamics with a salinity of 35,000 ppm over a period of 50 monitoring years. Overall, the plume does not significantly move outward after injection stops. Lower brine salinity may lead to the plume sinking downward as the difference between CO_2 density and brine density is not as significant as higher salinity.

At 80,000 ppm, the plume moves in a very similar manner to the base case (Figure 2-26). Although brine is more saline in this scenario, it is not enough to result in a noticeable change in the plume size. The range of salinity variation does not appear to strongly influence plume dynamics during the injection period.

Figure 2-27 shows that a salinity of 80,000 ppm does not vary the post-injection plume dynamics in any significant way. Although the brine density may now be higher than that of CO_2 compared to the base case, potentially leading to CO_2 migrating upward, that difference is hardly noticeable.

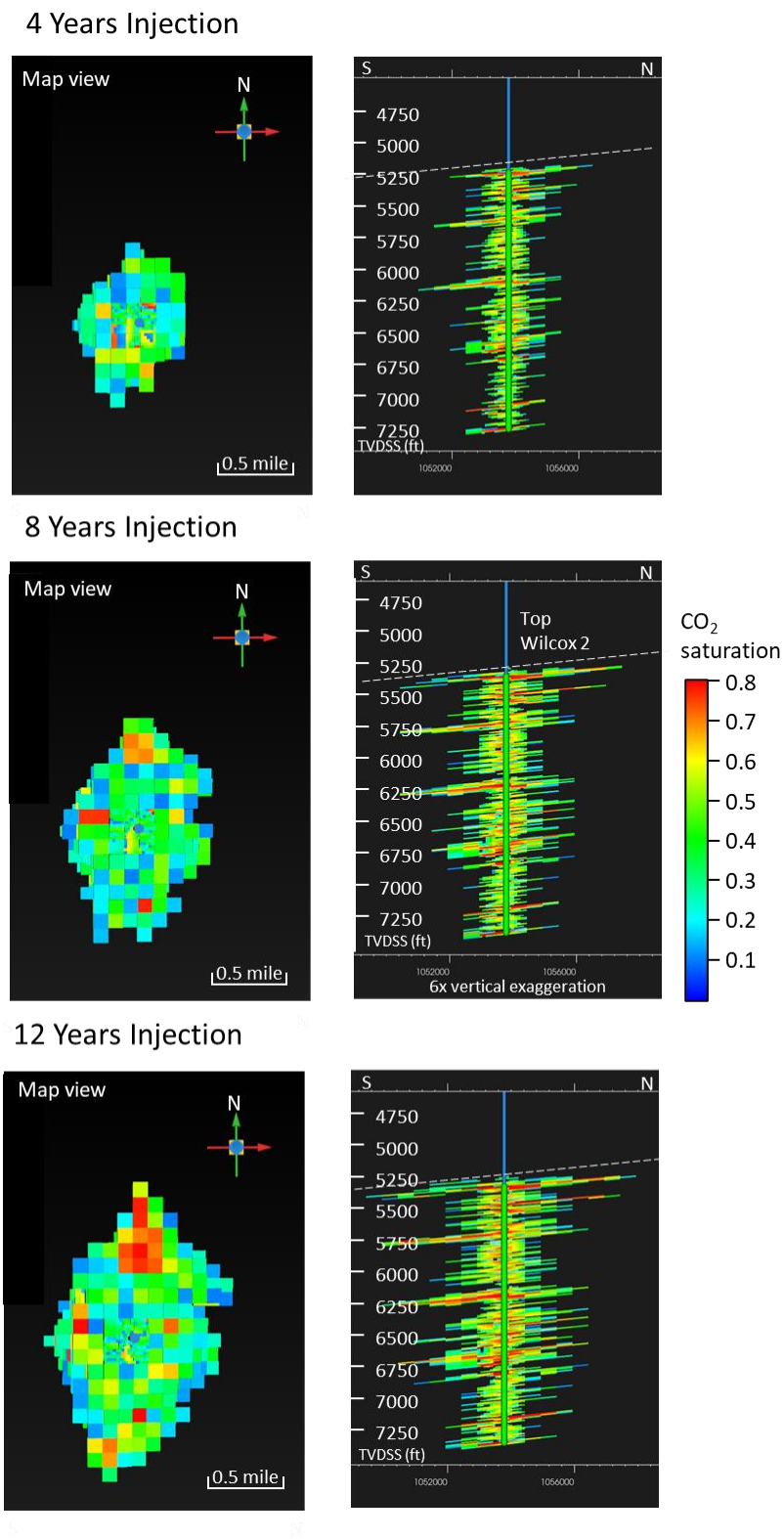

Figure 2-24: Map view of plume movement during injection period with 35,000 ppm brine salinity (left) and cross sectional view (right) of the CO_2 plume at 4, 8, and 12 years.

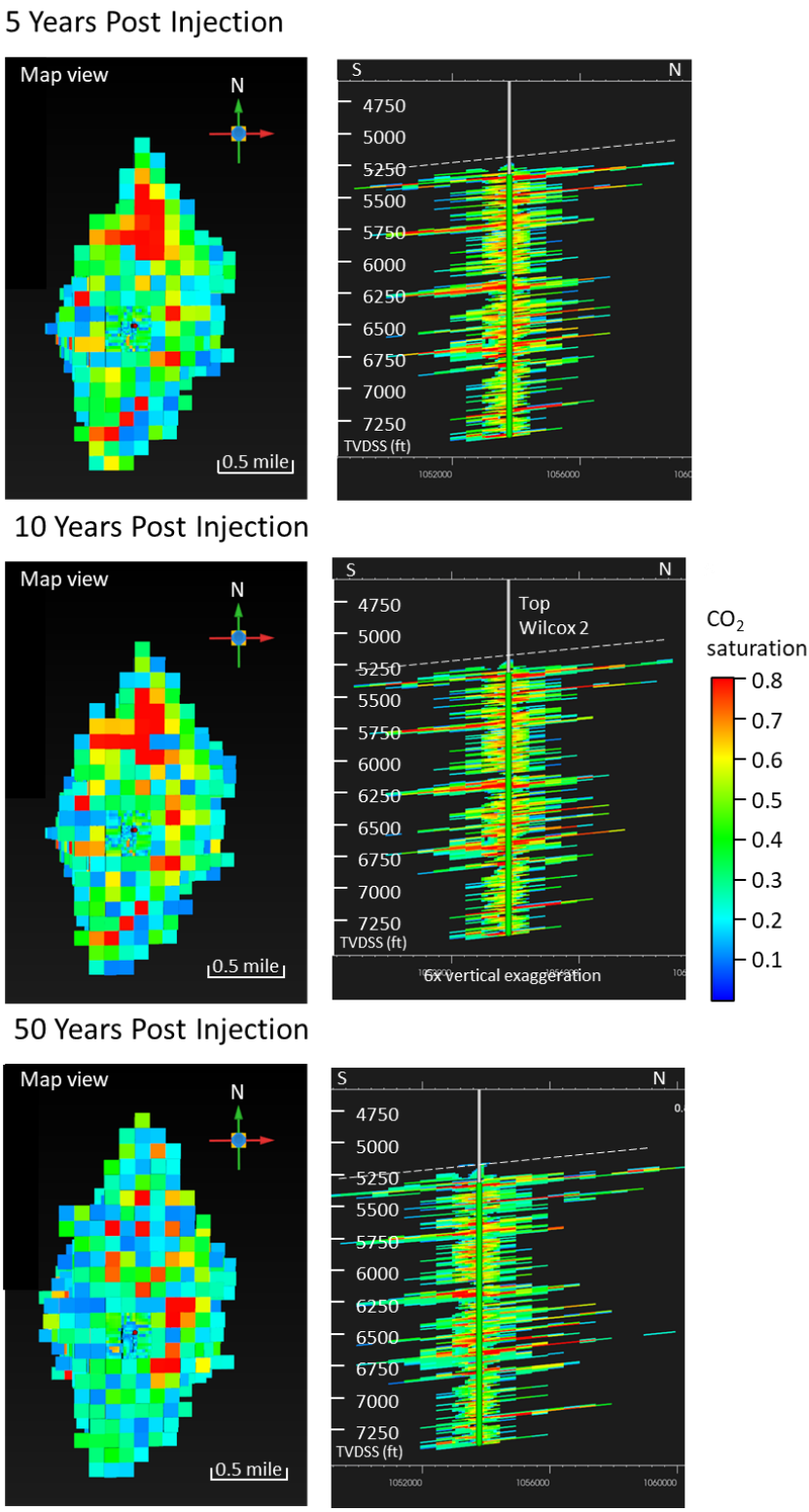

Figure 2-25: Map view of post-injection plume dynamics with 35,000 ppm brine salinity (left), and cross sectional view (right) of the CO_2 plume at 5, 10, and 50 years post-injection.

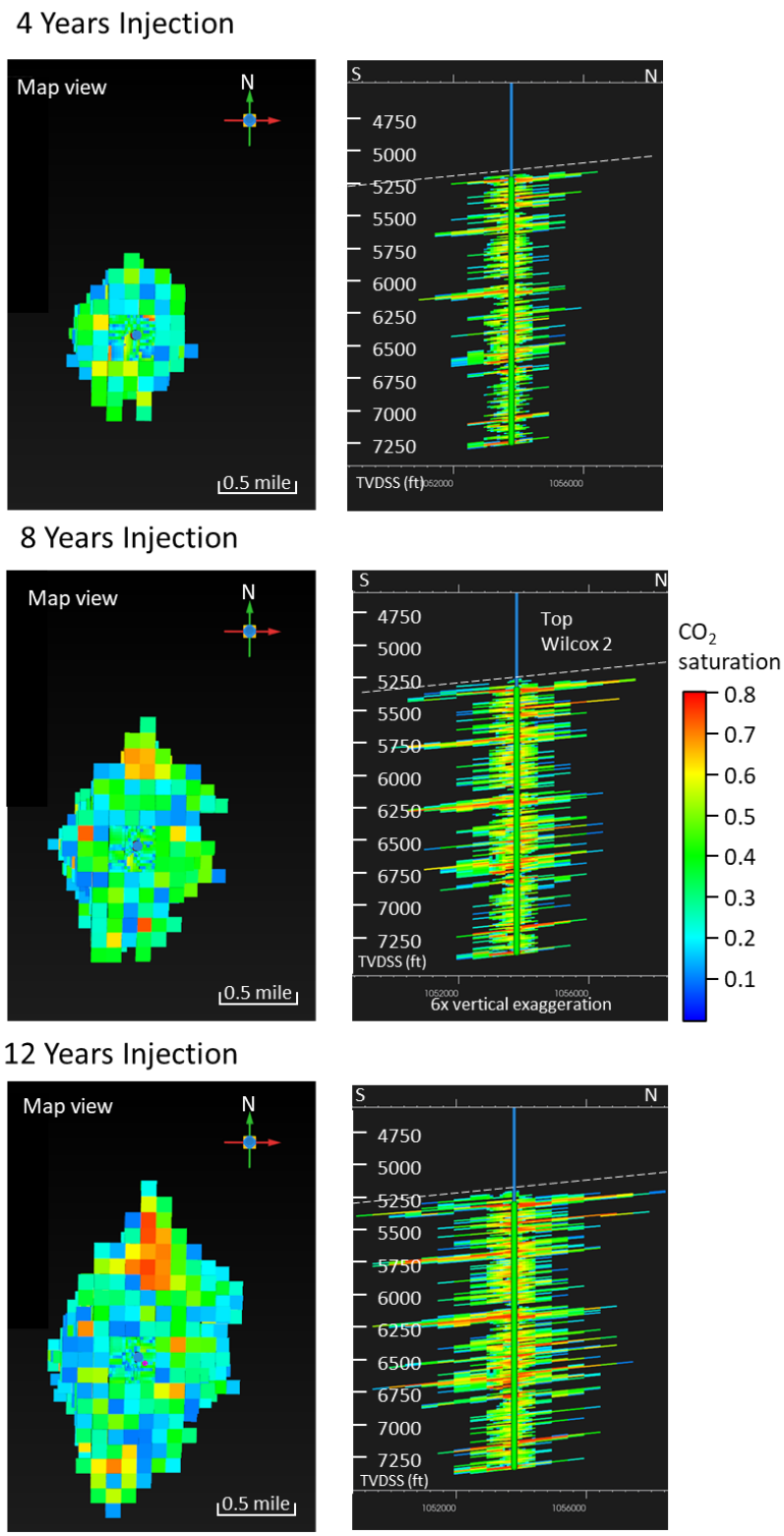

Figure 2-26: Map view of plume movement during injection period with 80,000 ppm brine salinity (left), and cross sectional view of the CO_2 plume at 4, 8, and 12 years (right).

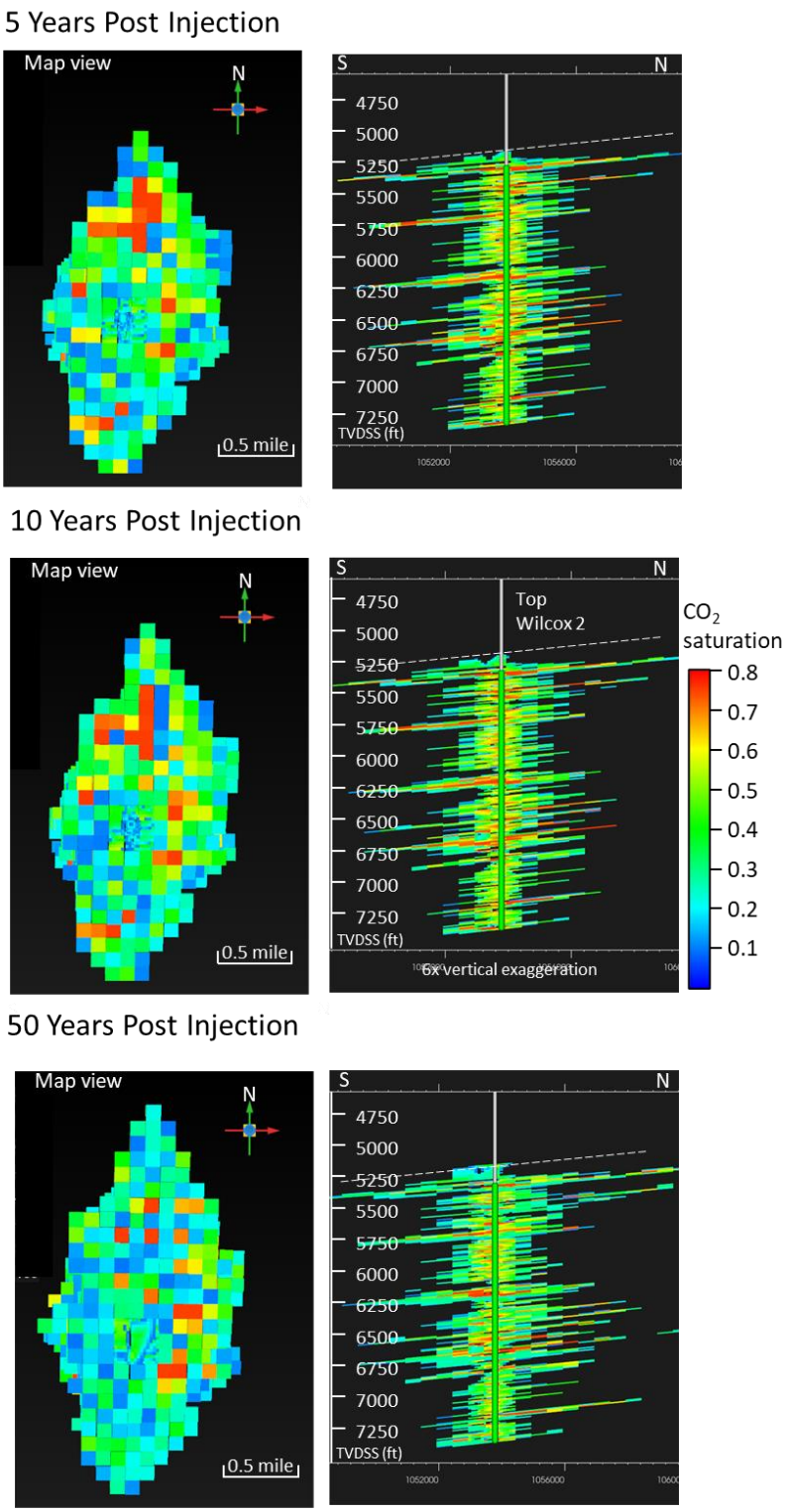

Figure 2-27: Map view of post-injection plume dynamics with 80,000 ppm brine salinity showing (left), and cross sectional view of the CO_2 plume at 5, 10, and 50 years post-injection (right).

Since the base case DRM employs a single set of relative permeability curves for both shale and non-shale facies due to a lack of measured data, it is likely that in reality, the shale relative permeability can be lower performing than its non-shale counterparts in our base case. A set of relative permeability curves with higher residual water saturation for shale facies has been adopted to experiment whether the influence would be significant on the plume movement and total injection. DRM results show that the plume is only slightly affected by this addition to the model in the Wilcox 2.

During injection, the north-south direction in which the plume propagates is still strongly influenced by the channel orientation (Figure 2-28). This is because the injection well penetrates a sand body inside a channel in this model, therefore it is less likely that the plume would encounter any significantly connected amount of shale facies and hence its relative permeability.

Figure 2-29 suggests that the post-injection plume is more likely to follow the high-permeability pathway along the channel and in the updip direction than to go through shale facies. However, this also makes the shale facies act more like baffles that flow would tend to go around. Because there is not a well-connected body of shale near the injection well in the model, the impact of the shale facies having its own relative permeability curves is rather limited.

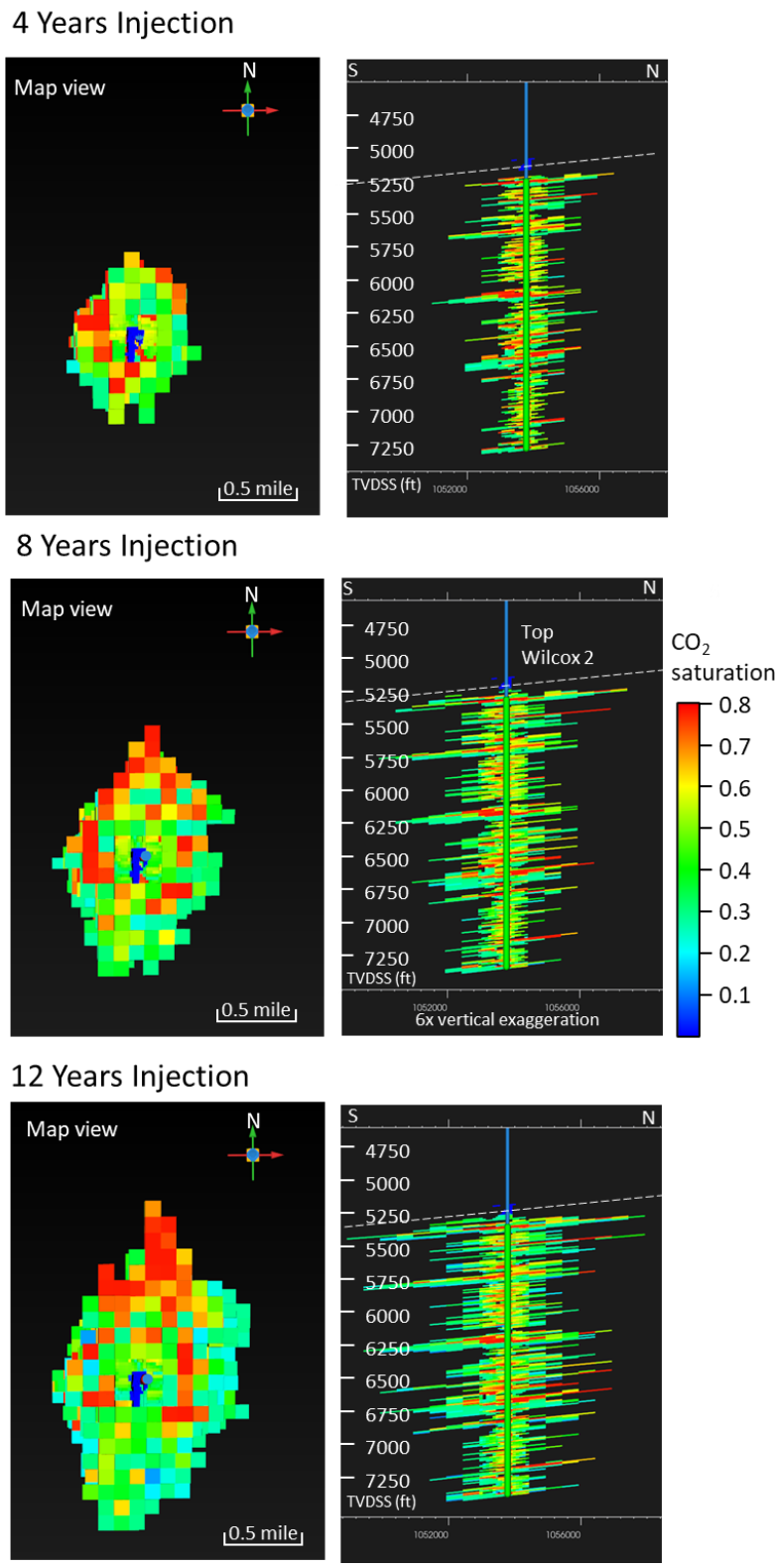

Figure 2-28: Map view of plume movement during injection period with multiple relative permeability curves (left), and cross sectional view of the CO_2 plume at 4, 8, and 12 years (right).

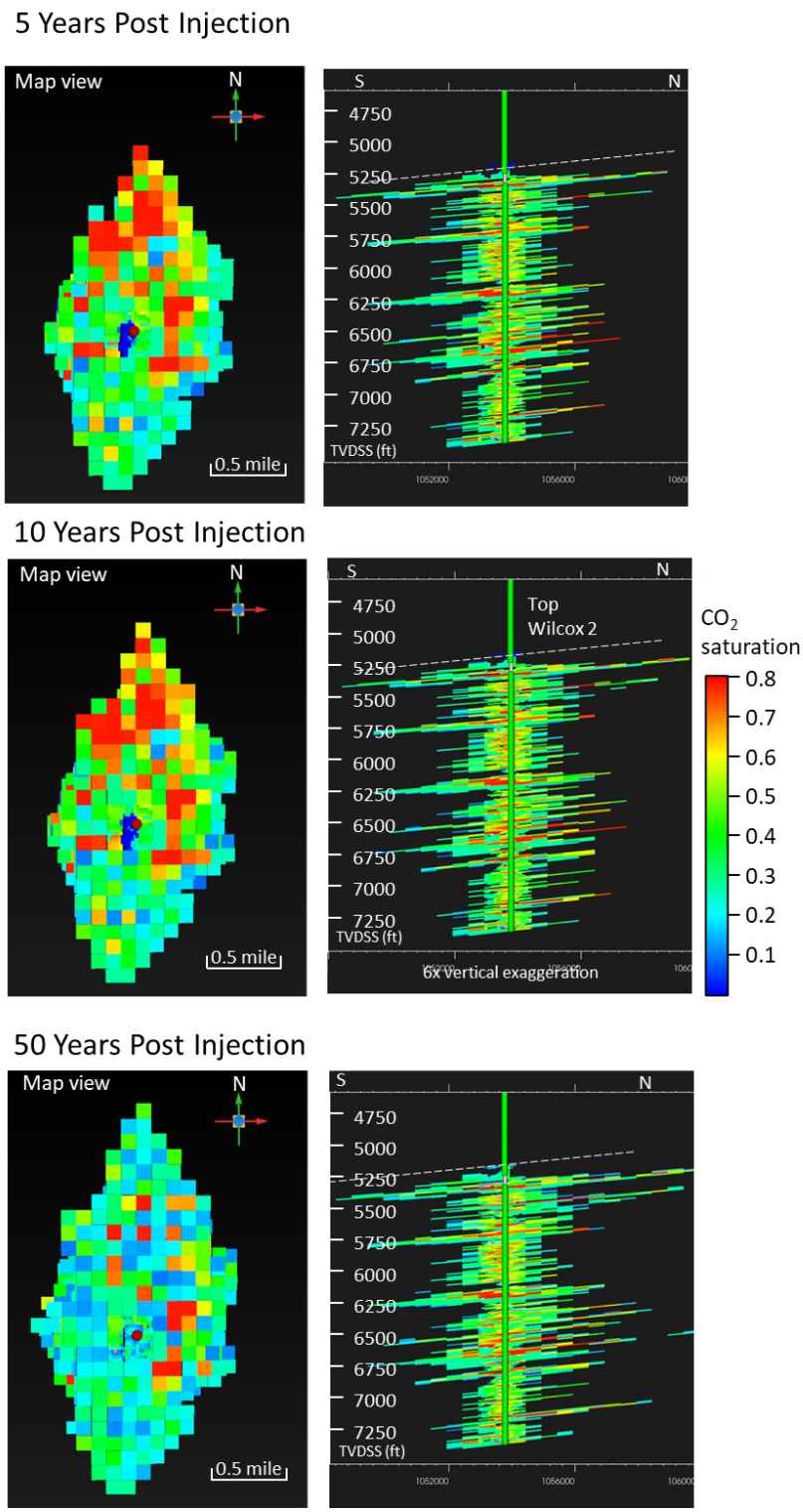

Figure 2-29: Map view of post-injection plume dynamics with multiple relative permeability curves (left), and cross sectional view of the CO_2 plume at 5, 10, and 50 years post-injection (right).